

# Development and Application of Laser-Collision Induced Fluorescence for Studying Dynamic and Structured Plasmas

64<sup>th</sup> AVS Symposium

Tampa, Florida November 2<sup>nd</sup> 2017

Edward V. Barnat

Sandia National Laboratories

Albuquerque, N.M., United States of America

*This work was supported by the Department of Energy Office of Fusion Energy Science  
Contract DE-SC0001939*



# Acknowledgements to the many collaborators that made these efforts succeed

## Post-doctoral researchers:

Kraig Frederickson (OSU) – Early development of LCIF

Brandon Weatherford (L3) – Application and development of LCIF

Ben Yee (SNL) and Ricky Tang (SNL) – Application and advancement of LCIF

Andy Fierro (SNL) – Kinetic simulations and radiation transport

## Visiting students:

B. Schiner (U. Iowa) – Anodic interfaces

Aimee Hubble (U. Michigan -> Aerospace Corp.)– Magnetized interfaces

## Collaborators:

Matt Hopkins (SNL) – Kinetic simulations

Scott Baalrud (U. Iowa) – Anode interface physics

John Foster (U. Michigan) – Plasma generation and plasma transport.

Vlaidimir Kolobov (CFDRC) – Physics of positive column discharges

Andy Xiong and Mark Kushner (U. Michigan) – FIW simulations

Peter Bruggeman (U. Minnesota) – High pressure plasma physics



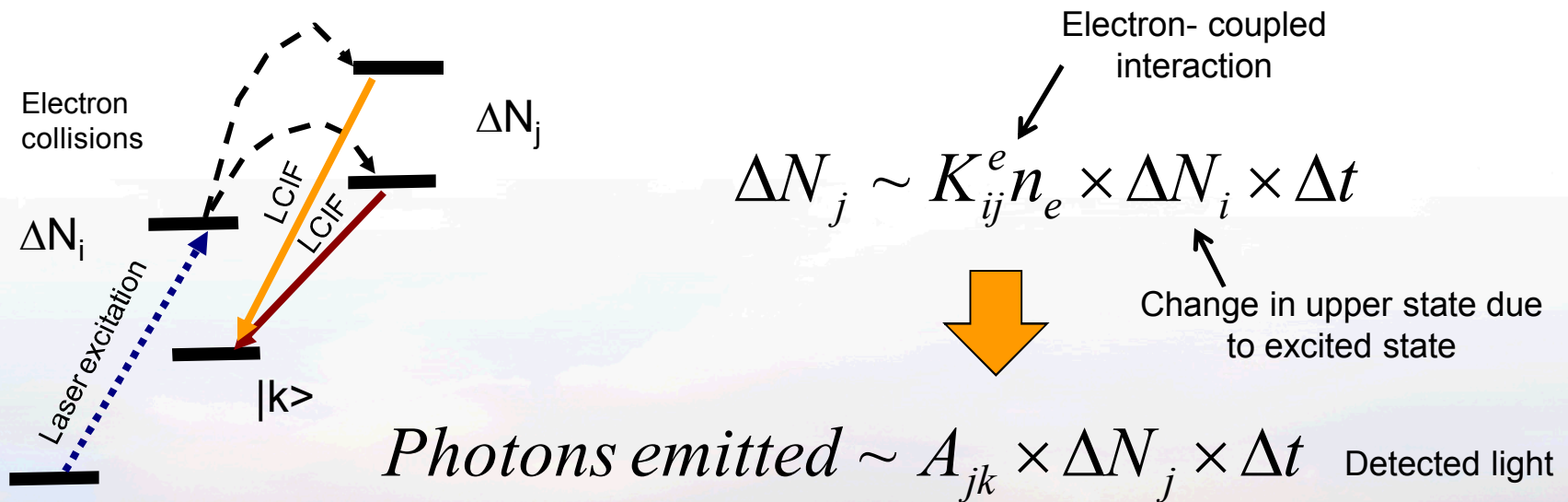
# Laser-collision induced fluorescence provides measure of electron density and "temperature"

- **Motivation: What is the density? What is the temperature? Where and When?**
  - Two-dimensional snap-shots of density provide insight into plasma physics.
- **In this presentation**
  - Part I: Laser-collision induced fluorescence (LCIF) primer
    - Overview of the LCIF technique
    - Physics that governs LCIF and trends predicted by this physics
  - Part II: Implement and benchmark technique
    - Experimental setup
    - Time evolution of LCIF and time integrated LCIF
  - Part III: Applications of LCIF:
    - Dynamic and structured plasmas
  - Part IV: Future directions and concluding comments
    - Atmospheric pressure LCIF



# LCIF is based on redistribution of excited state by plasma species (electrons)

- Pulsed laser excitation populates an intermediate state
  - Relaxation processes deplete excited state
- Portion of excited state population gets redistributed into "uphill" states
  - Driven by interaction with energetic plasma species (electrons).



**LCIF looks for changes in emission of neighboring states after laser excitation**

# Redistribution of laser excited states can be a complex process

- A "good" model is required to predict transfer between levels.
  - Employ a collisional-radiative model (CRM) to predict redistribution of
- Sets of coupled equations scale with the number of states needed to be accounted for.
  - Uncertainties will scale with the number of unknowns
  - Limit sets of interactions that are "most likely" going to impact system response

*"Photon mixing"*

*"Electron mixing"*

*"Neutral mixing"*

$$\frac{dN_j}{dt} = \left[ \sum_{i>j} A_{ij} N_i - \sum_{i<j} A_{ji}^j N_j \right] + \left[ \sum_{i \neq j} K_{ij}^e N_i - \sum_{i \neq j} K_{ji}^e N_j \right] n_e + \sum_k \left[ \sum_{i \neq j} K_{ikj}^a N_i - \sum_{i \neq j} K_{jki}^a N_j \right] N_k$$

Absorption  
and  
emission

Excitation into and  
out of states

Redistribution

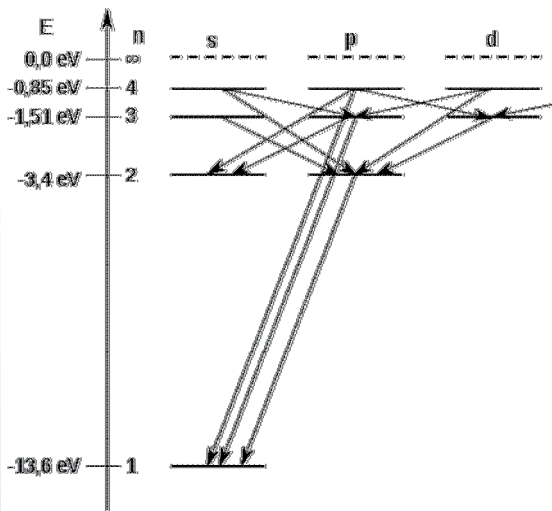


# Complexity of many atomic systems

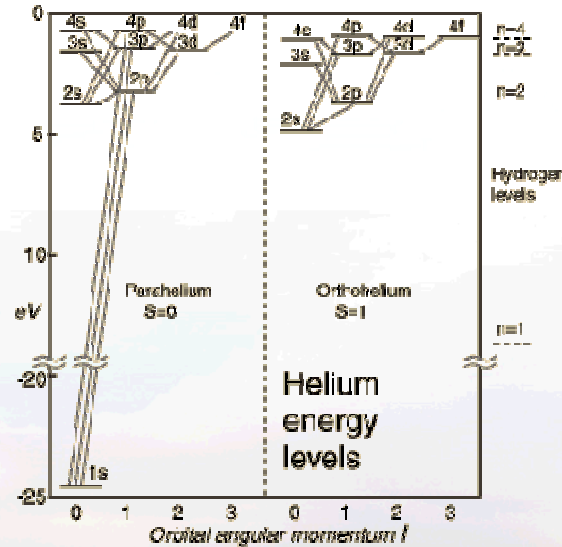
## LCIF "challenging"

- Atomic structure will govern which pathways are accessible for LCIF
  - Which states radiate, and are they uniquely detectable

### Hydrogen

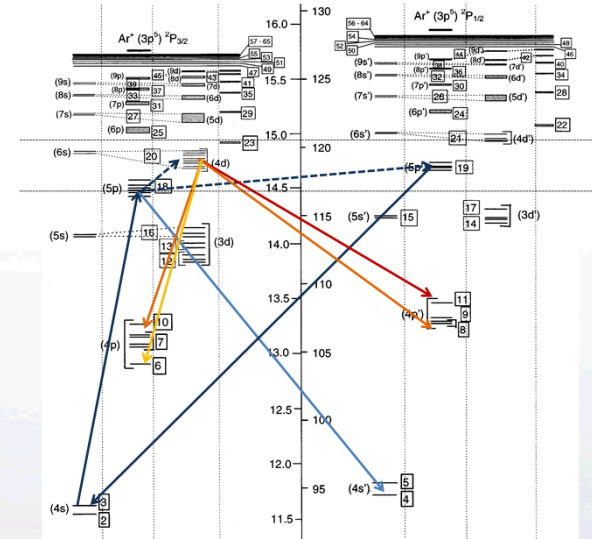


### Helium



<http://hyperphysics.phy-astr.gsu.edu/hbase/quantum/helium.html>

### Argon



Taken from Bogeaerts et. al, J. Appl. Phys. **84**, 121, 1998

[http://commons.wikimedia.org/wiki/File:Grotrian\\_H.svg](http://commons.wikimedia.org/wiki/File:Grotrian_H.svg)

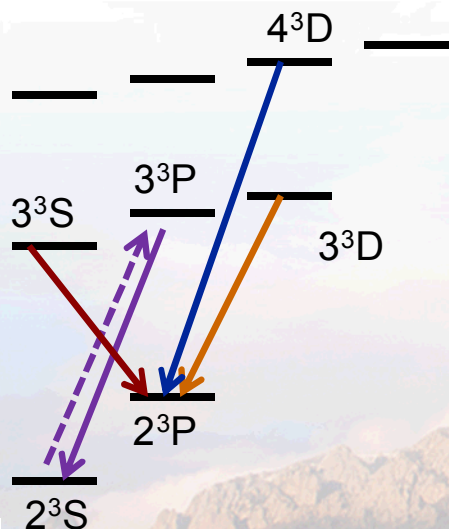
*The number of interactions that need to be accounted for scales with complexity of the system*



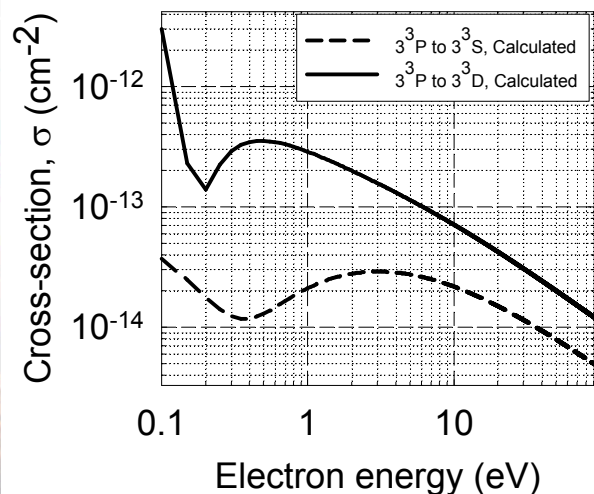
# Helium atom serves as target species for LCIF measurements

- **Limited excitation/ de-excitation pathways.**
  - Hydrogen is simpler, but restricted pathways.
  - Neon, Argon, etc... more complex structure.
- **Cross-sections between states are well known.**
  - Inter-state transitions between high lying states are “known” for helium.
  - Utilize functionalized form of cross-sections compiled by Ralchenko<sup>1</sup>

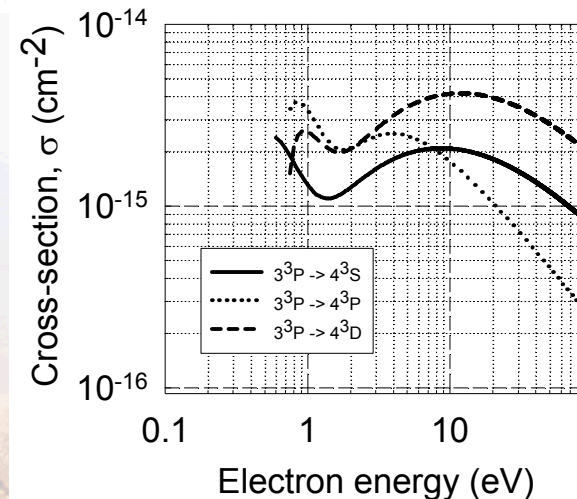
## Key transitions



## $3^3P \rightarrow 3^3S, 3^3D$



## $3^3P \rightarrow 4^3S, 4^3P, 4^3D$



**Principles extend to other systems**

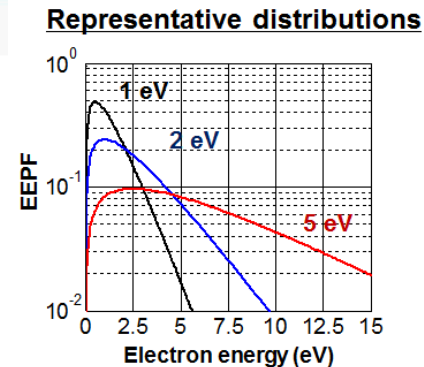
Sandia National Laboratories



# Electron-induced collision rates are computed from cross-sections and electron distribution functions

- Functional dependence of collision rates are computed as a function of “effective” electron temperature
  - Explicit dependence on EEPF will influence these curves

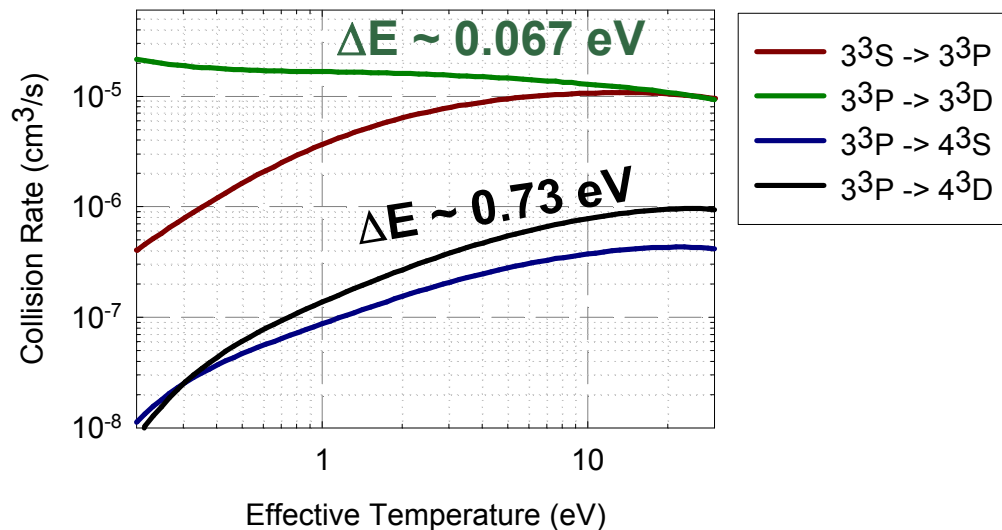
$$K_{ij}^e = \langle \sigma_{ij}(E) v_e(E) f(E) \rangle$$



## Key transitions



## Key Rates

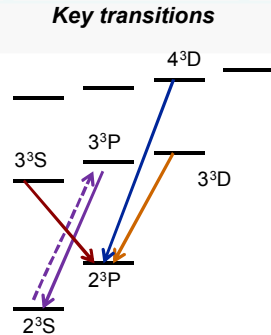


**Barrier between states plays key role in population transfer processes**

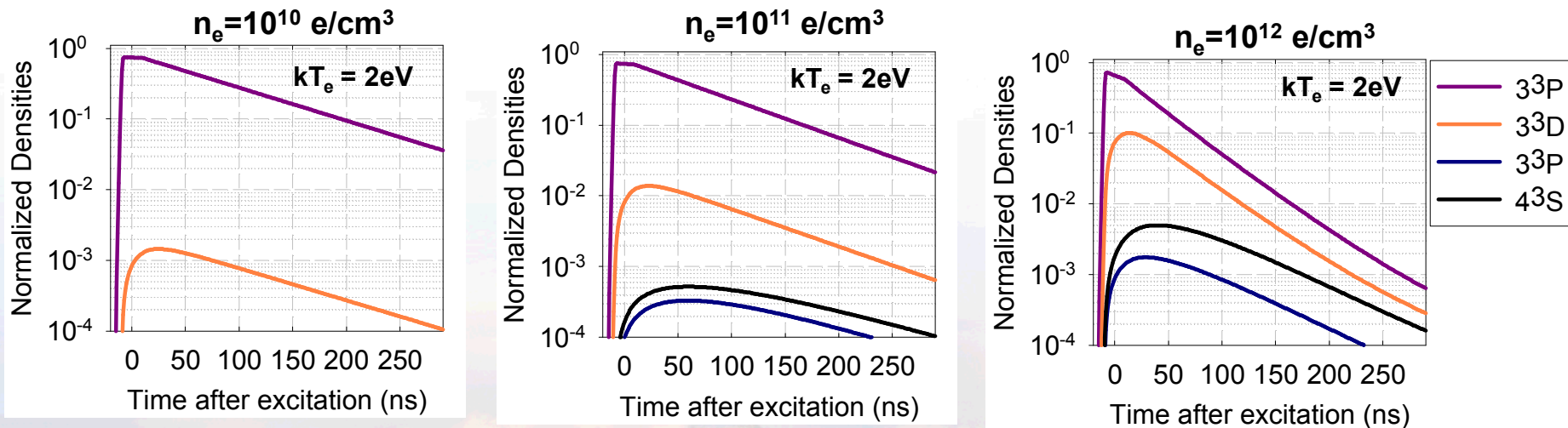


# Electron-induced collisions are observable in energetically “up hill” transitions

- Solution of the CRM including both electrons and radiative decay.
  - Electrons redistribute excited state to near by states
- There are two key-observables obtained from these simulations
  - Degree of re-distribution scales with collision rate ( $n_e, T_e$ )
  - Lifetime of excited states become truncated at higher densities ( $K \times n_e \sim A$ )



## Representative state populations after excitation

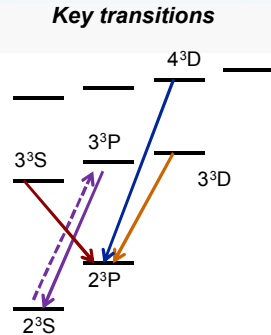


*Temporal integration of light detected serves to simplify LCIF implementation*

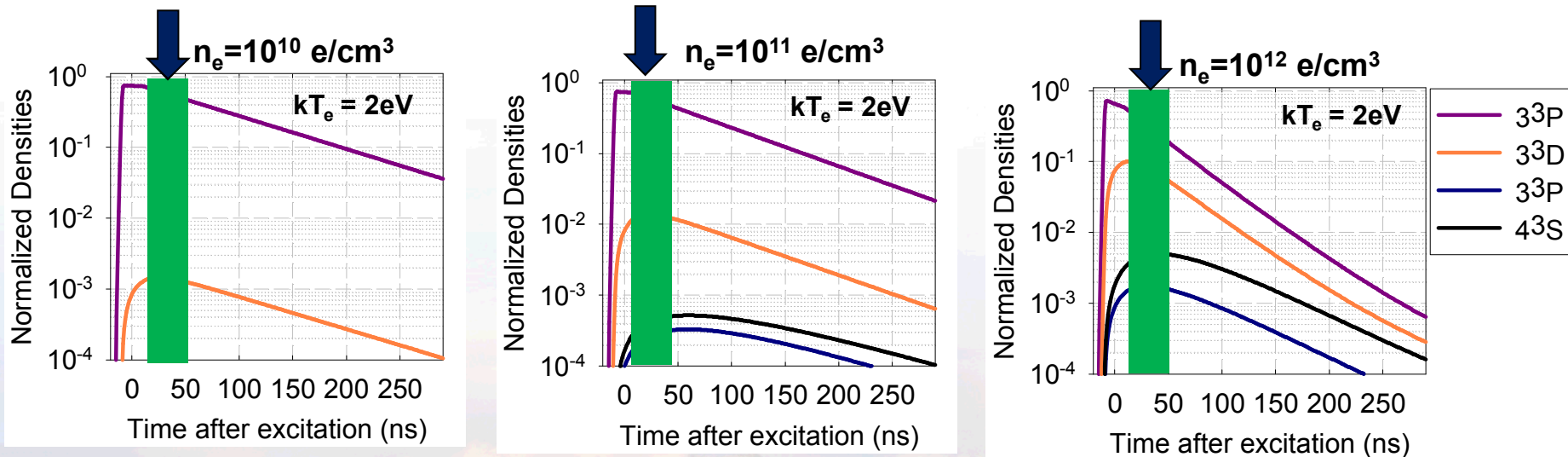


# Electron-induced collisions are observable in energetically “up hill” transitions

- Solution of the CRM including both electrons and radiative decay.
  - Electrons redistribute excited state to near by states
- There are two key-observables obtained from these simulations
  - Degree of re-distribution scales with collision rate ( $n_e, T_e$ )
  - Lifetime of excited states become truncated at higher densities ( $K \times n_e \sim A$ )



## Representative state populations after excitation



*Temporal integration of light detected serves to simplify LCIF implementation*



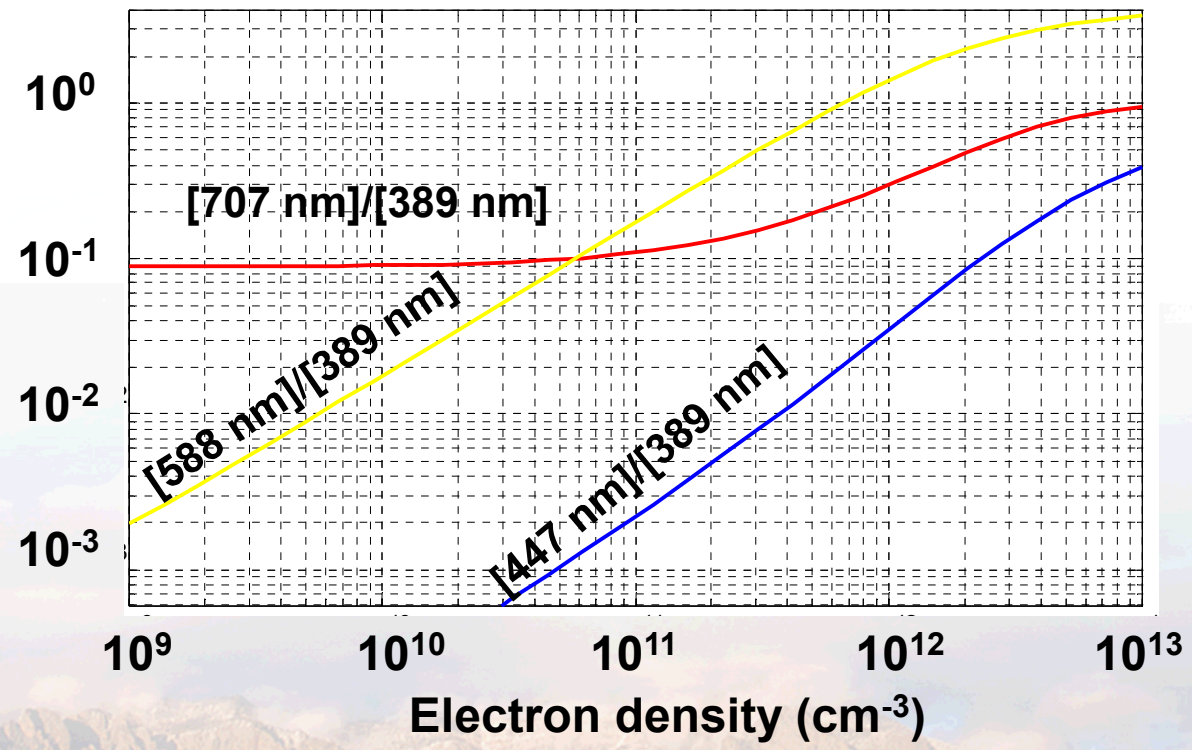
# Ratio of LCIF to LIF yields electron induced excitation rates

- Ratios constructed from LCIF and LIF from the laser excited state yields rates
  - Eliminated dependence of exact knowledge of how much excited state was generated

## Ratio between LCIF and LIF

$$\frac{\Delta N_j}{N_{3^3P}} \sim K_{3^3P \rightarrow j}^e n_e \times \Delta t$$

## Ratio of LCIF to 389 nm LIF



*Provides a direct measure of  $n_e$  if  $K$  is independent of  $T_e$*



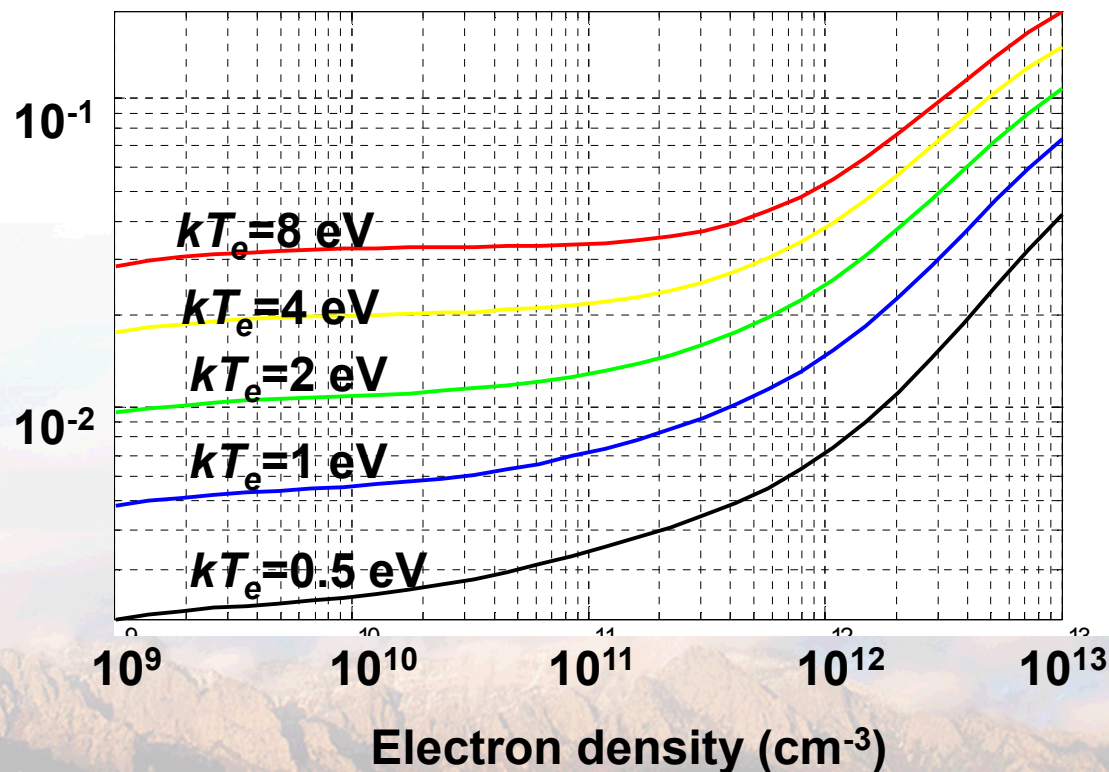
# Ratios of various LCIF lines can serve as a measure of effective temperature

- Ratios constructed from two LCIF measurements yields ratio of two rates
  - Elimination of electron density dependence.

Ratio between two LCIF signals

$$\frac{\Delta N_j}{\Delta N_i} \sim \frac{K_{0j}^e}{K_{0i}^e}$$

Ratio [447 nm]/[588 nm]



# Laser-collision induced fluorescence provides measure of electron density and "temperature"

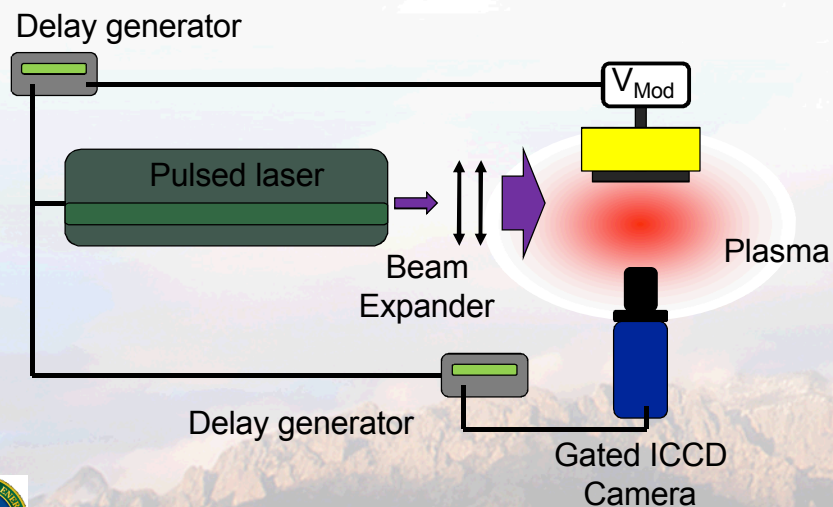
- **Motivation: What is the density? What is the temperature? Where and When?**
  - Two-dimensional snap-shots of density provide insight into plasma physics.
- **In this presentation**
  - Part I: Laser-collision induced fluorescence (LCIF) primer
    - Collisional-radiative model used to predict LCIF
    - Physics that governs LCIF
  - **Part II: Implement and benchmark technique**
    - **Experimental procedures**
    - **Demonstration of LCIF for various implementations**
  - Part III: Applications of LCIF:
    - Dynamic and structured plasmas
  - Part IV: Future directions and concluding comments
    - Atmospheric pressure LCIF



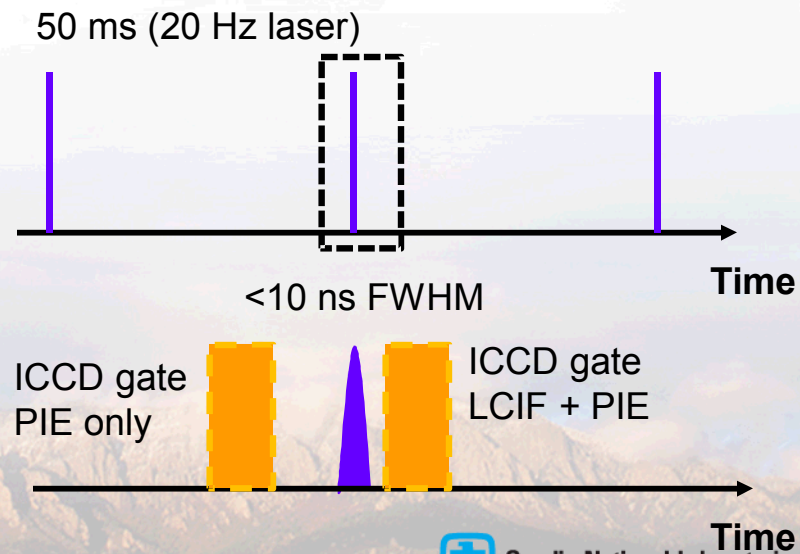
# Experimental implementation of the LCIF is realized

- **Nanosecond pulsed laser used for excitation**
  - $< 10$  ns FWHM,  $< 0.1$   $\text{cm}^{-1}$  line width
- **Timing of experiment controlled by delay generators**
  - Move experiment and imaging with respect to firing of the laser
- **Image LCIF with gated-intensified CCD**
  - Narrow ( $\sim 5$  nm FWHM) interference filters centered on lines of interest
- **Take two images per transition considered**
  - Total emission and plasma induced emission (PIE) - subtract the two

## Optical setup



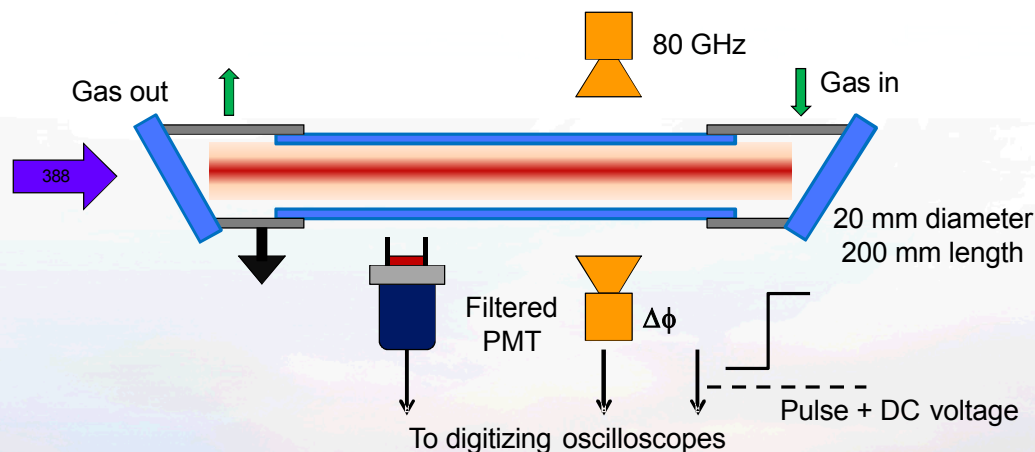
## Timing sequence



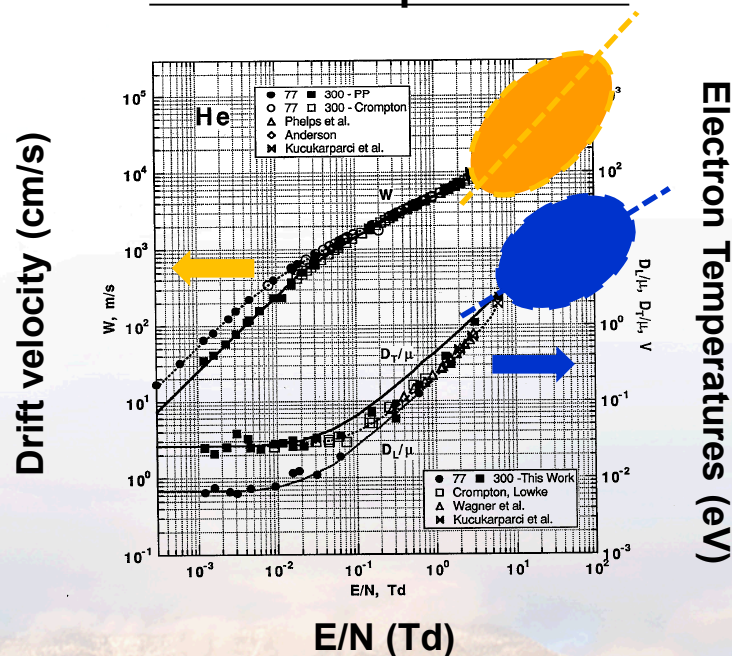
# Pulsed positive column is utilized to benchmark LCIF technique

- Pulse discharge currents generate broad density range
  - ~ 10 Microseconds, 80 GHz interferometer
- Compute drift velocities and extract electron temperatures
  - Use published drift parameters

## Positive column



## Helium drift parameters

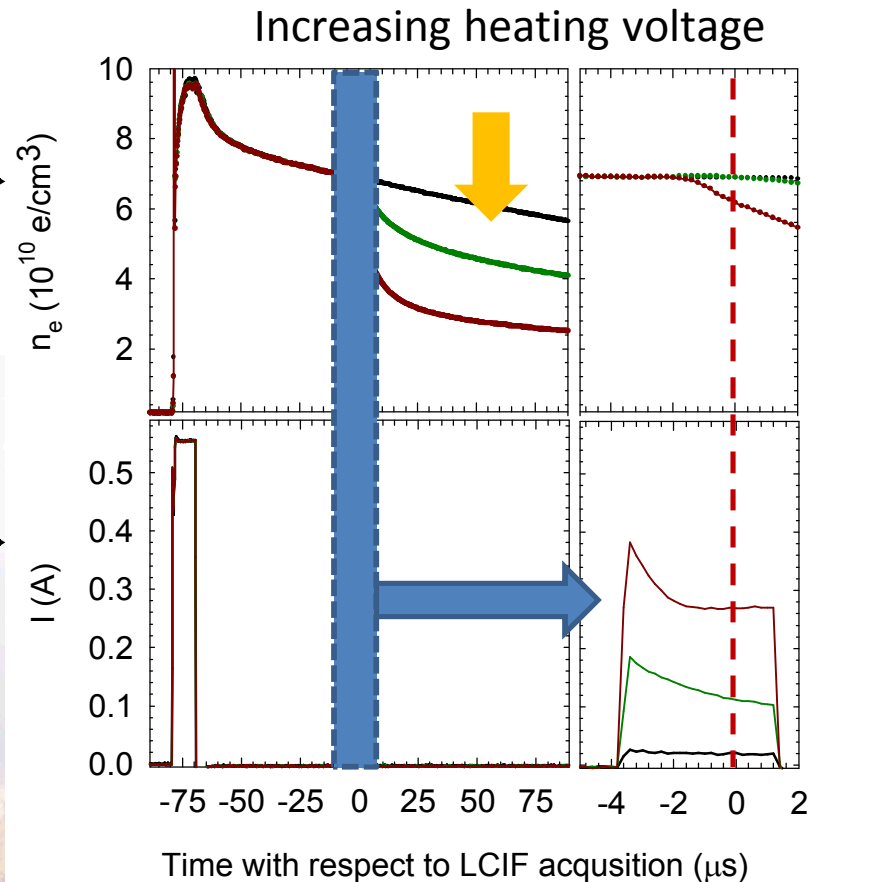
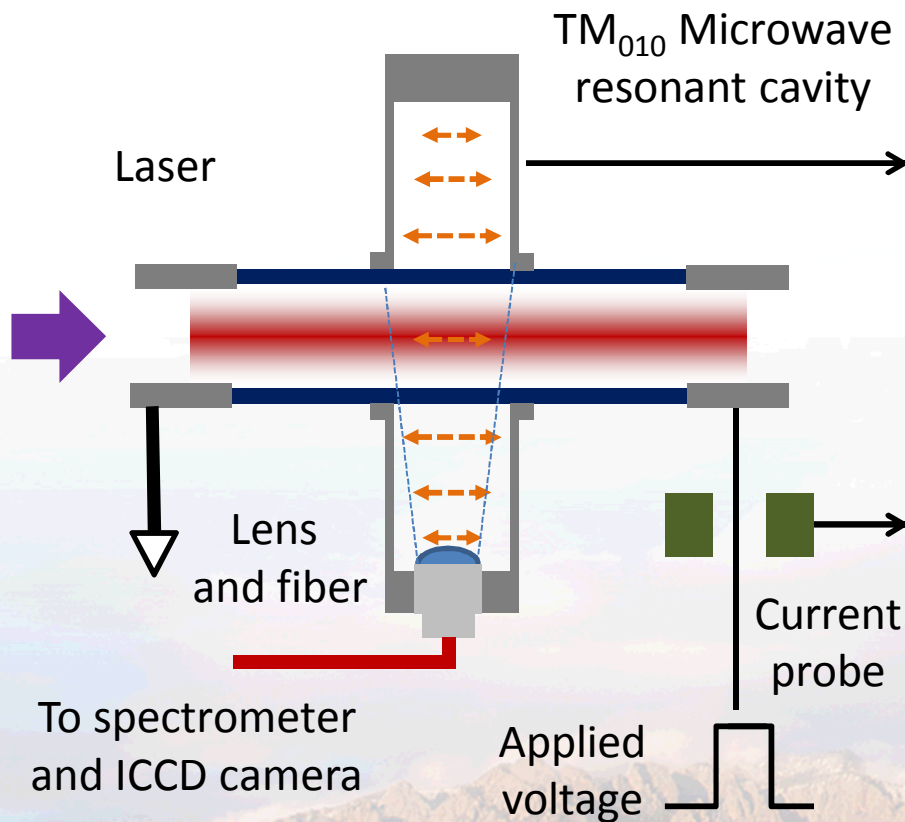


*Positive column is a good vehicle to benchmark LCIF technique*



# (Double) Pulsed positive column is utilized to benchmark LCIF technique

- Double pulse method controls plasma parameters ( $n_e$ , " $T_e$ ")
  - First pulse generates plasma, second pulse "heats plasma"

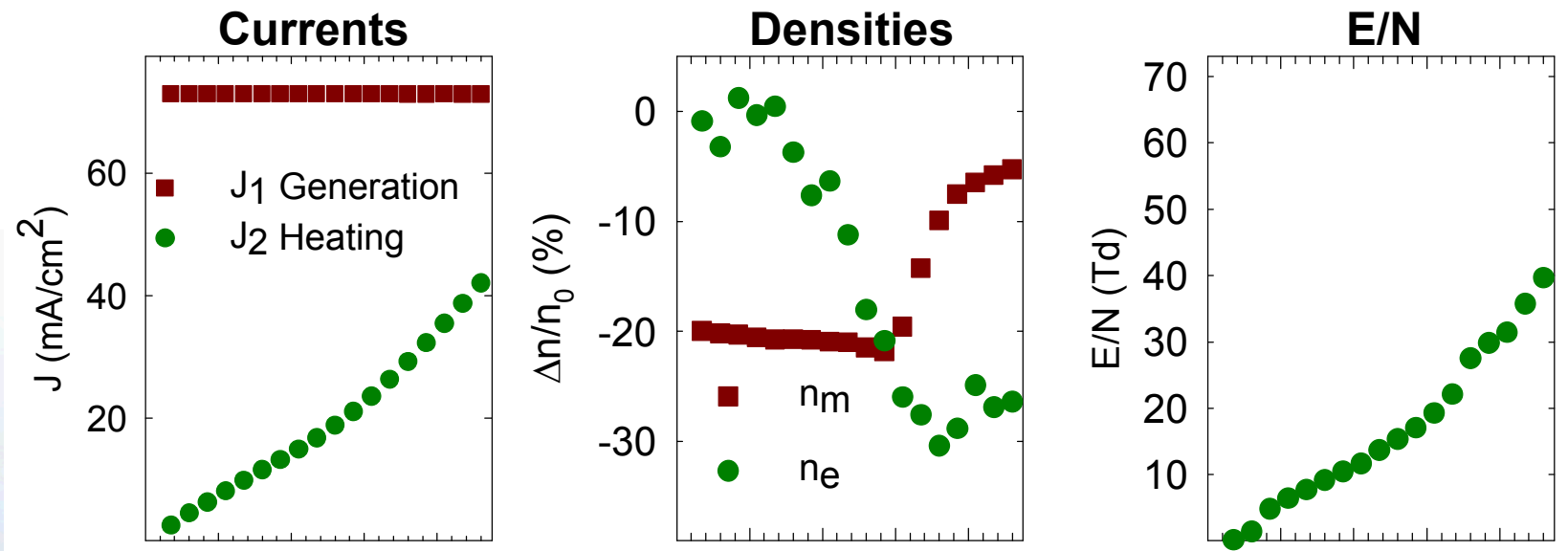


# E/N is manipulated with applied heating voltage

- Published drift parameters are utilized to correlate drift velocities to E/N
  - Excitation and ionization compliments analysis.

## Time averaged parameters

5  $\mu$ s average, 10  $\mu$ s after pulse is applied



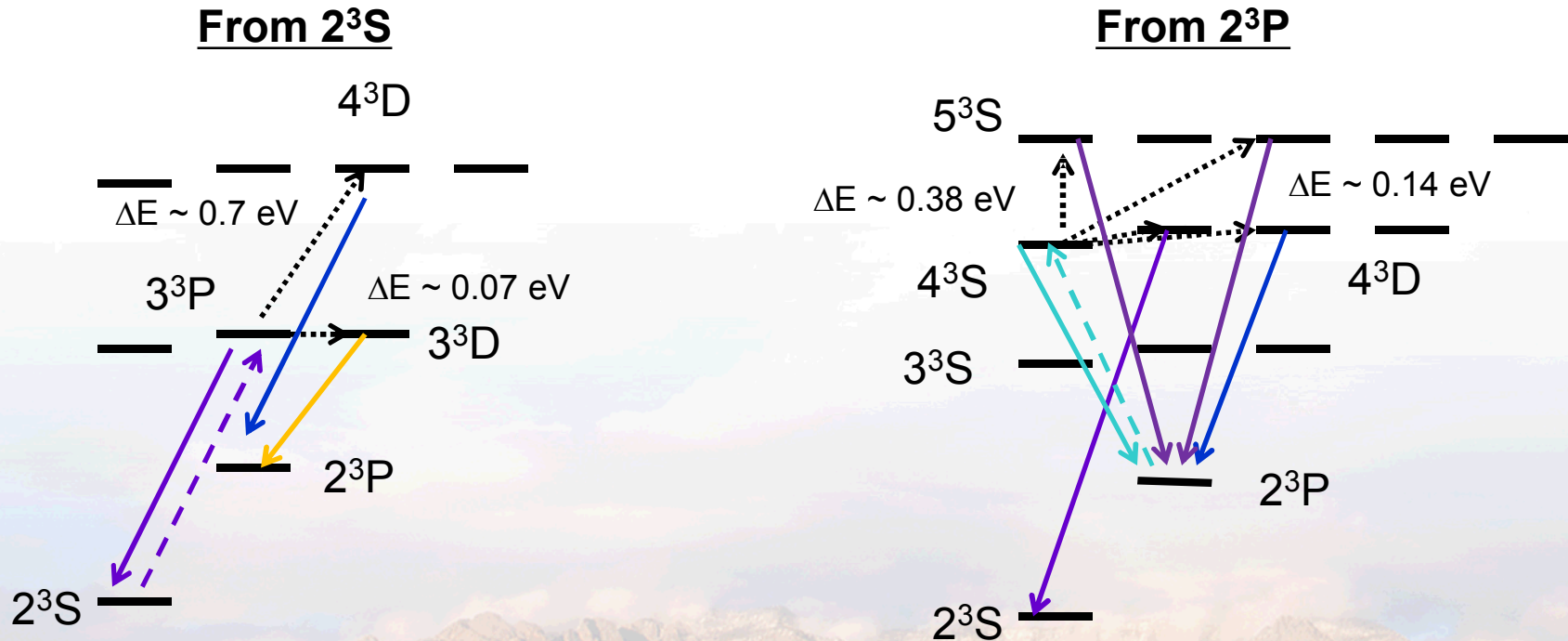
Applied "heating" voltage

*Good control over E/N with application of the second pulse*



# Spectroscopic pathways interrogated for helium

- Lower base density of  $2^3P$  advantageous, but some tradeoffs
  - Lose the nice "temperature free"  $3^3P \rightarrow 3^3D$  transition
  - Spectrally dense - many transitions  $\sim 400$  nm



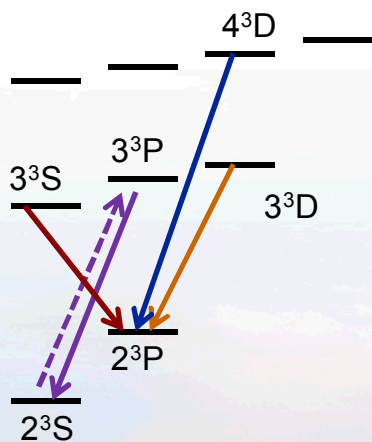
*Choice depends on optical thickness and density of probed state*



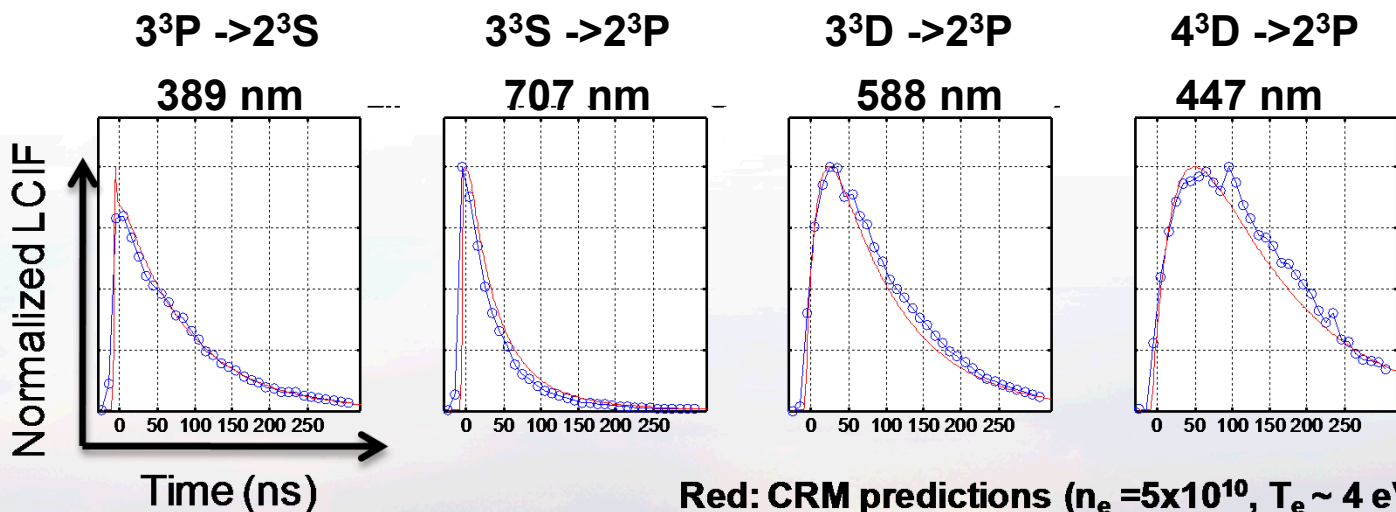
# First steps: Verify time resolved LCIF to test CRM

- Excite the  $2^3S - 3^3P$  transition @ 389 nm
  - Monitor LIF back to  $2^3S$
  - Monitor LCIF from  $3^3D$  and  $4^3D$
- Compare measured results to simulated results

## Key transitions



## Representative results



Red: CRM predictions ( $n_e = 5 \times 10^{10}$ ,  $T_e \sim 4$  eV)  
Blue: Measured LIF/LCIF

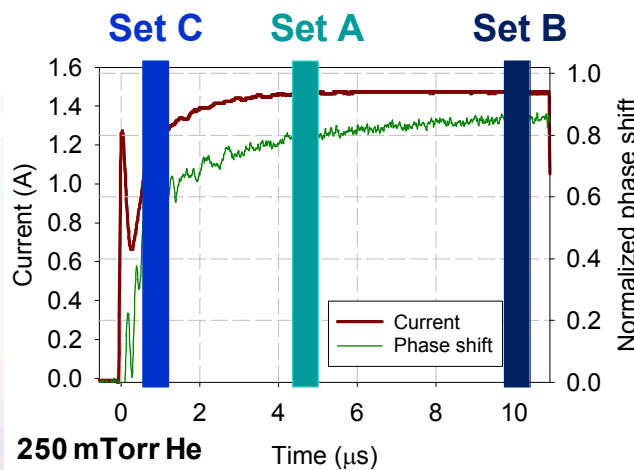
*Capturing time-resolved trends is key for benchmarking LCIF*



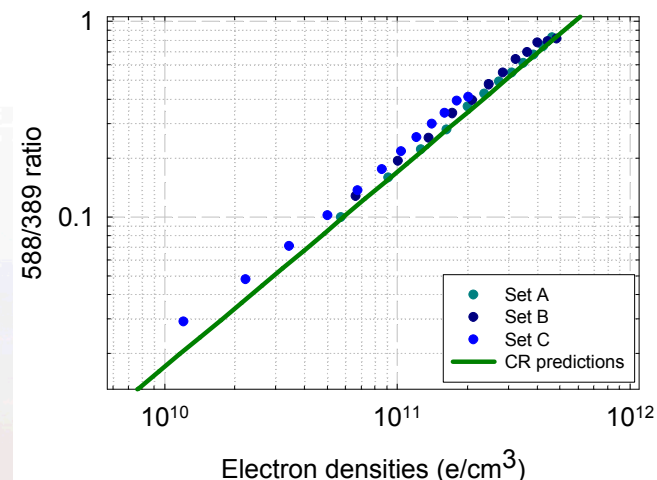
# [588]/[389] ratio exhibits linearity over nearly two orders of magnitude

- Better yet, measured ratios agree reasonably well with computed ratios
  - Slightly higher, and some deviation at low density
- Examined trends at different times during the current pulse
  - Anticipate different temperatures as column is established

### Waveforms during excitation



### Density dependent ratio trends

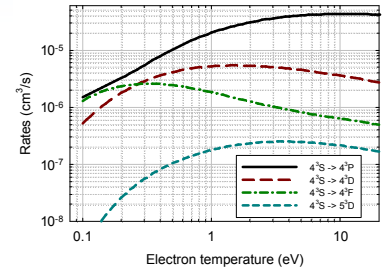


*Density measurements obtained at different times essentially overlay each other*

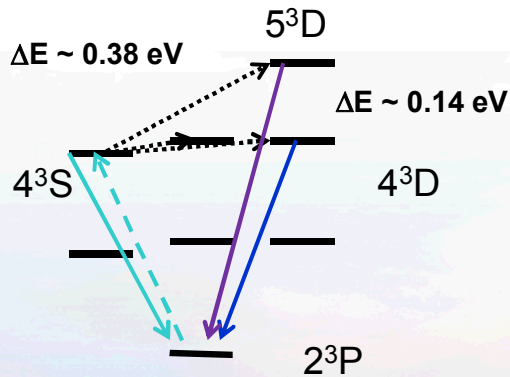


# $2^3P$ excitation pathway is also benchmarked

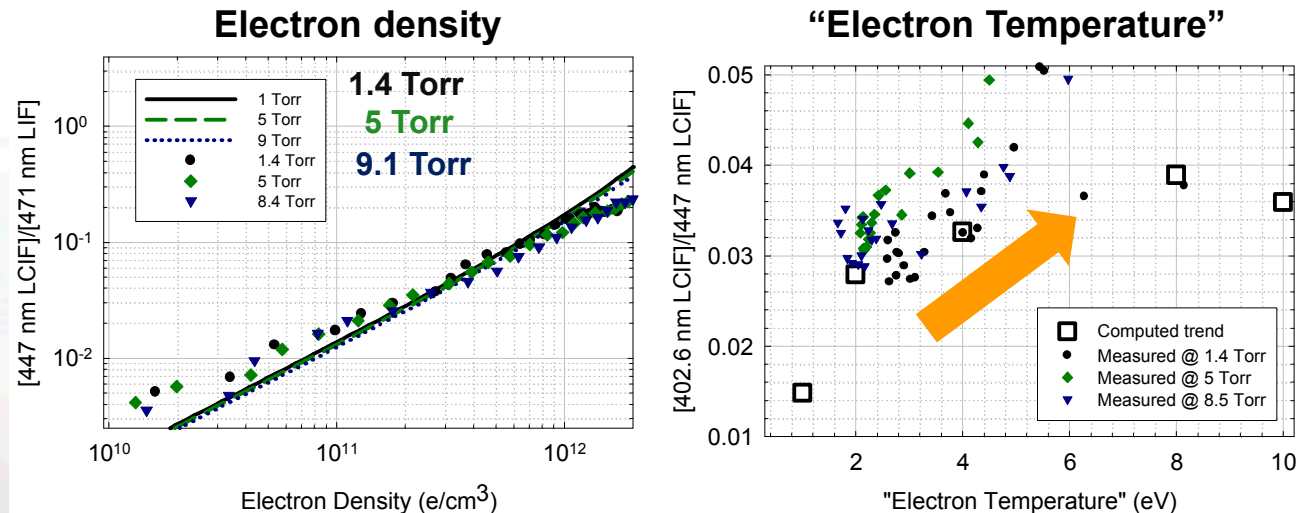
- Utilize simple set of coupled equations to compute evolution of the system
  - Not self consistent, but sidesteps many unknowns
  - Rely on functional forms of excitation cross sections<sup>[1]</sup>



## Spectroscopic pathway



## Key Scaling Trends



**Electron density trends gas pressure for modest pressures**

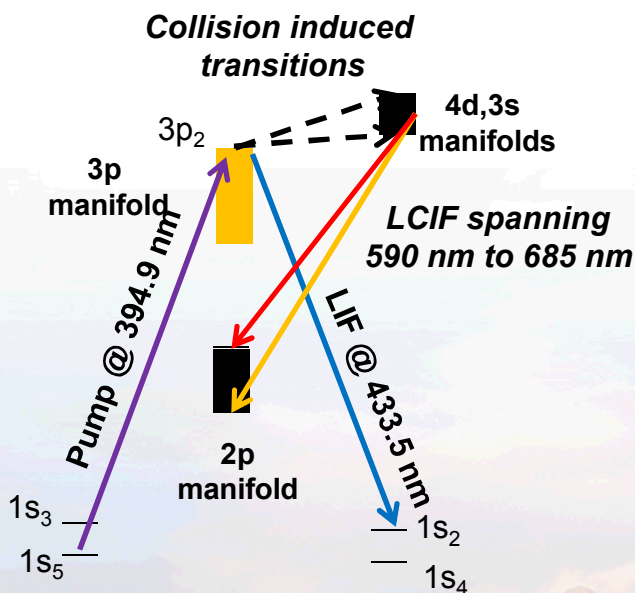


<sup>[1]</sup> Yu. Ralchenko, R. K. Janev, T. Kato, D. V. Fursa, I. Bray, F. J. De Heer, Atomic Data and Nuclear Data Tables **94**, 603 (2008).

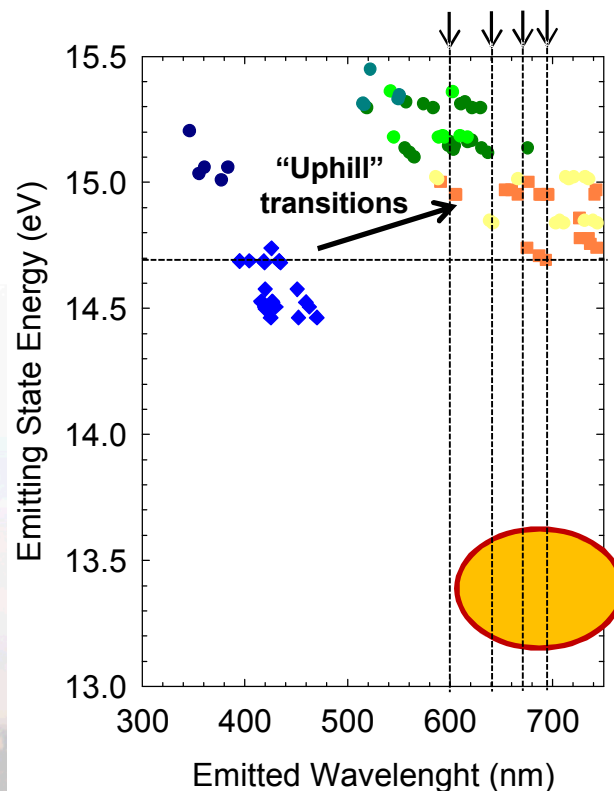
# Complexity of Argon manifold offers choice for LCIF implementation

- Well-chosen excitation scheme is important for successful implementation
  - Excite the upper ( $3p_2$ ) states and look for collisional coupling into higher ( $3s$ ,  $4d$ ,  $5d$  ...) states.

## Proposed pathway



## Target transitions



Target transitions	Wavelength (nm)	A ( $\times 10^6 \text{ s}^{-1}$ )	$\Delta E$ (eV)
$1s_5 \rightarrow 3p_2$	394.9	0.46	0
$3p_2 \rightarrow 1s_4$	404.6	0.04	0
$3p_2 \rightarrow 1s_3$	418.2	0.56	0
$3p_2 \rightarrow 1s_2$	433.5	0.39	0
<hr/>			
$4d_5 \rightarrow 2p_{10}$	687.13	2.8	0.024
$4s_1'' \rightarrow 2p_7$	688.82	0.25	0.265
$4s_1' \rightarrow 2p_7$	687.96	0.18	0.268
<hr/>			
$4d_3 \rightarrow 2p_{10}$	675.28	1.9	0.055
$4s_1'' \rightarrow 2p_6$	676.66	0.4	0.316
<hr/>			
$3s_5 \rightarrow 2p_{10}$	641.63	1.2	0.152
$3s_4 \rightarrow 2p_{10}$	638.47	0.42	0.161
$3s_2 \rightarrow 2p_8$	643.16	0.05	0.335
$5d_3 \rightarrow 2p_6$	630.77	0.60	0.450
$5d_6 \rightarrow 2p_7$	636.49	0.56	0.413
$5d_5 \rightarrow 2p_6$	636.96	0.42	0.431
$3s_2 \rightarrow 2p_{10}$	638.47	0.42	0.161
<hr/>			
$4s_1'' \rightarrow 2p_{10}$	591.21	1.05	0.316
$3s_3 \rightarrow 2p_{10}$	588.26	1.2	0.327
$3s_1 \rightarrow 2p_{10}$	586.03	0.29	0.335
$4s_5 \rightarrow 2p_9$	588.86	1.29	0.494
$4s_4 \rightarrow 2p_8$	592.8812	1.10	0.498
$5s_1'' \rightarrow 2p_6$	583.42	0.52	0.609
$4s_3 \rightarrow 2p_4$	597.1601	1.10	0.671

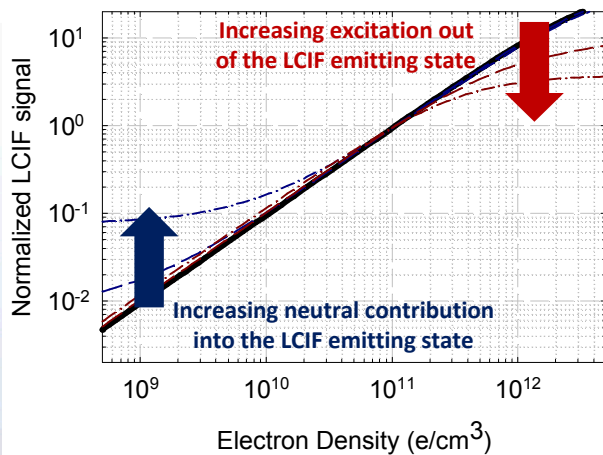
Pump  
Monitor  
LCIF

Other excitation pathways also can be chosen

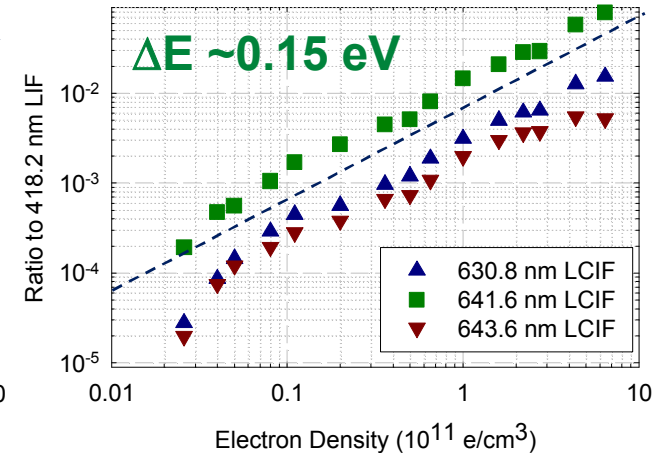
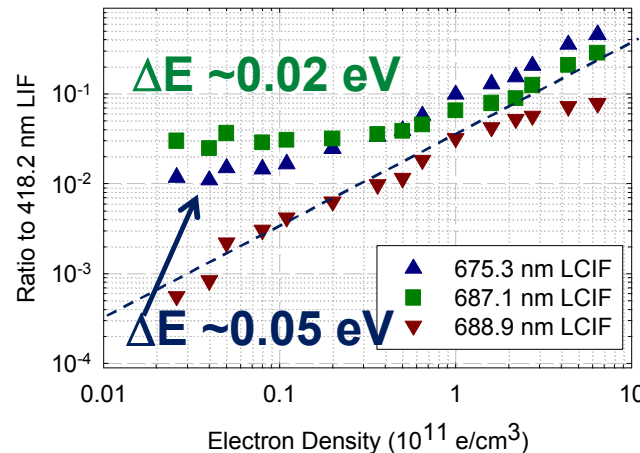
# Electron density scaling demonstrated for select transitions

- Simple model is utilized to assess LCIF scaling.
  - Include neutral collisions and excitation into and out of target states.
- LCIF emanating from energetically uphill states is measured as a function of electron density.
  - Fixed E/N by tuning generating voltage pulse.

## Anticipated scaling



## Observed scaling



*Good linearity with electron density for higher lying states*



# E/N Scaling likewise demonstrated for select transitions

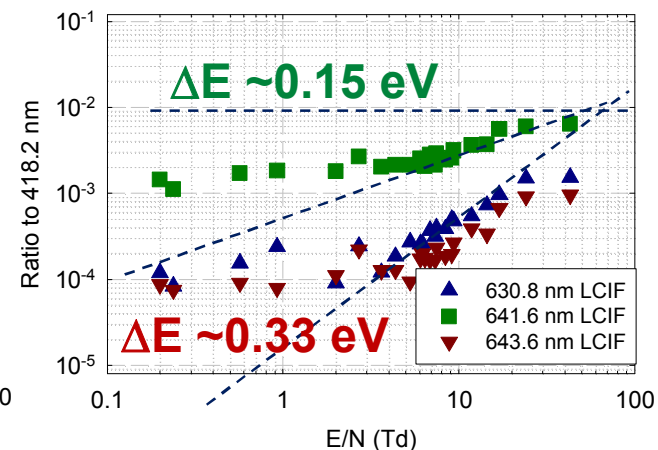
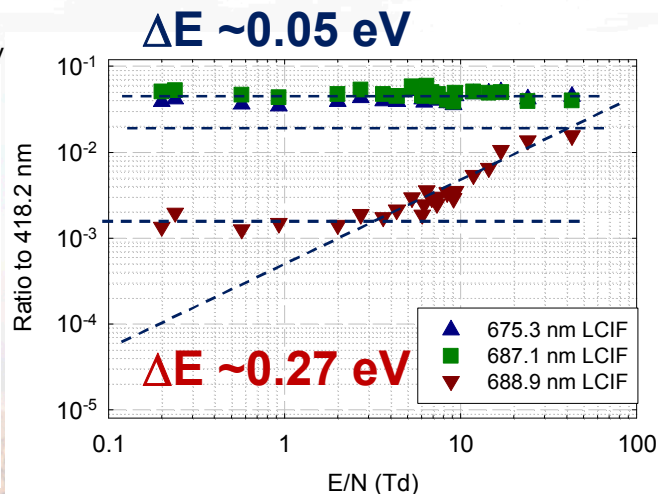
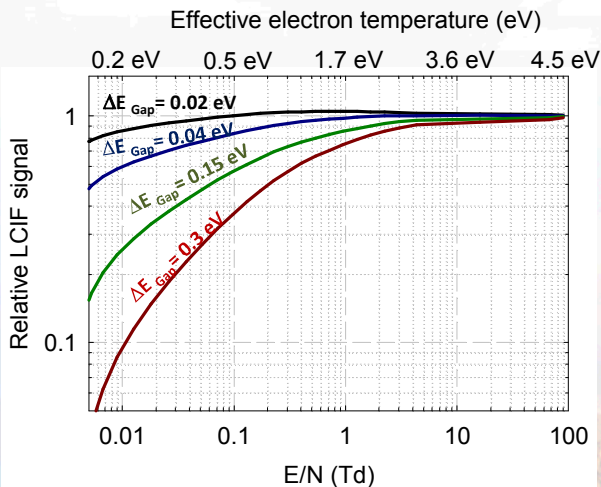
- Cross-sections not well known, assume functional form

$$\sigma(E) = 4\pi a_0^2 \alpha \left(\frac{E}{\Delta E}\right)^n \left(\frac{E}{\Delta E} - 1\right) \ln\left(1.25\beta \frac{E}{\Delta E}\right)$$

- LCIF emanating from energetically uphill states is measured as a function of E/N at fixed density.
  - Residual E/N remaining due to ambipolar fields regulating losses.

## Anticipated scaling

## Observed scaling



Good range of transitions that demonstrate different E/N sensitivities



# Laser-collision induced fluorescence provides measure of electron density and "temperature"

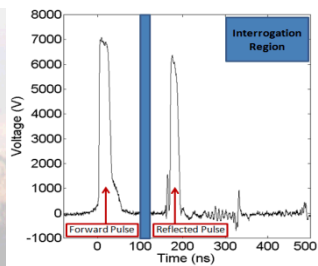
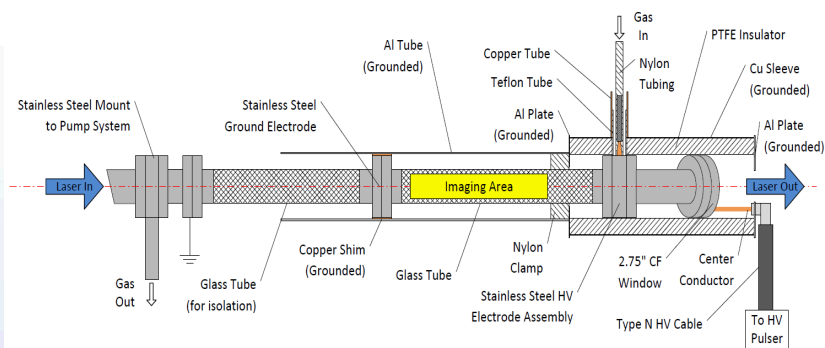
- **Motivation: What is the density? What is the temperature? Where and When?**
  - Two-dimensional snap-shots of density provide insight into plasma physics.
- **In this presentation**
  - **Part I: Laser-collision induced fluorescence (LCIF) primer**
    - Collisional-radiative model used to predict LCIF
    - Physics that governs LCIF
  - **Part II: Implement and benchmark technique**
    - Experimental setup
    - Time evolution of LCIF and time integrated LCIF
  - **Part III: Applications of LCIF:**
    - **Dynamic and structured plasmas**
  - **Part IV: Future directions and concluding comments**
    - Atmospheric pressure LCIF



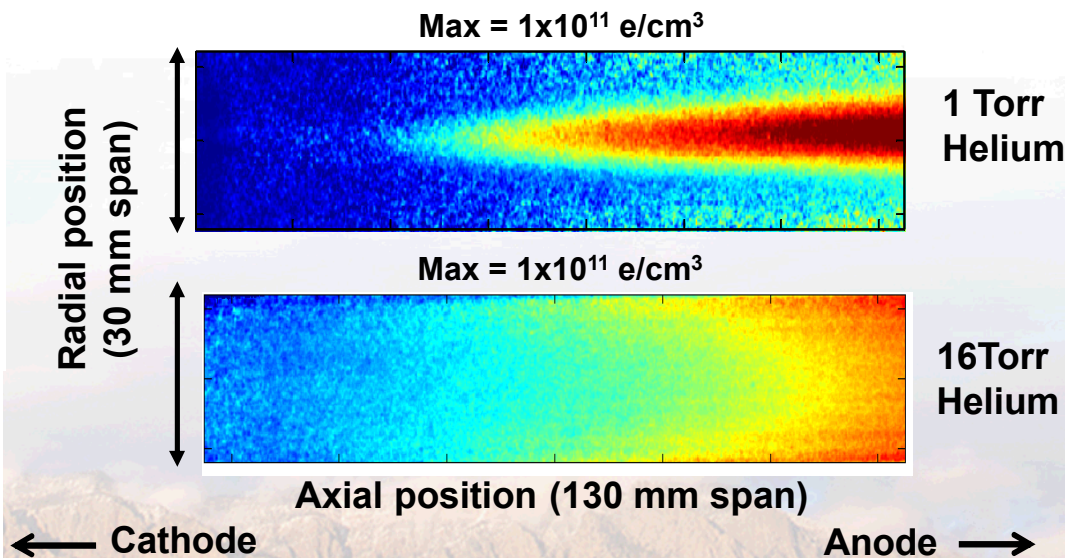
# Studies were performed to assess properties of FIW generated plasmas

- Fast-ionization waves (FIW) have been the subject of interest in the PSC.
  - High voltage (many kV), short pulse (10's ns) excitation.
  - Large E/N (100's Td) lead to efficient plasma formation.
- Earlier studies examined the plasma distribution immediately (~50 ns) after the FIW propagated. (B. Weatherford).
  - Laser (collision) induced fluorescence used to map plasma species.

## Setup



## Measured electron densities

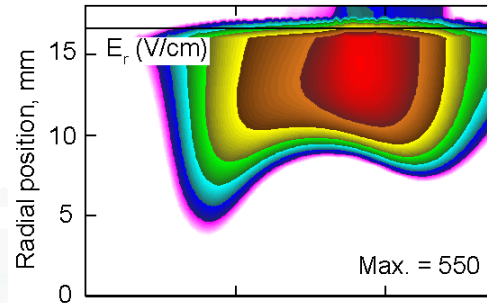


# Changes in excitation are due to concentration of electric field

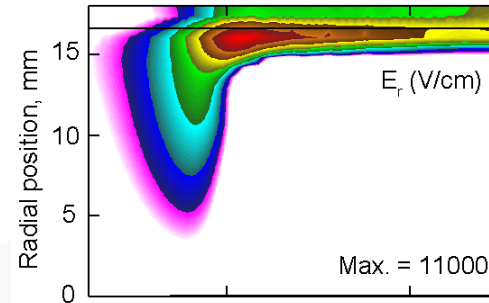
- Electric fields are simulated to become stronger and more localized at higher pressures (A. Xiong, M. Kushner).
  - Energy deposition becomes more confined to the walls due to strong electric fields.

Radial field

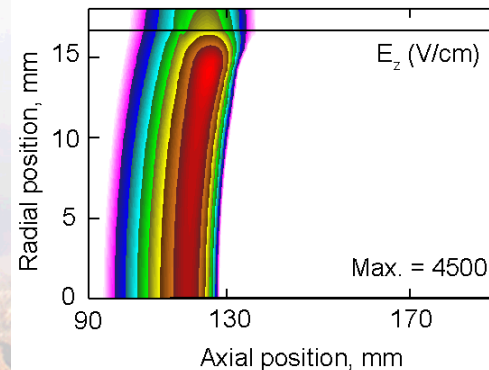
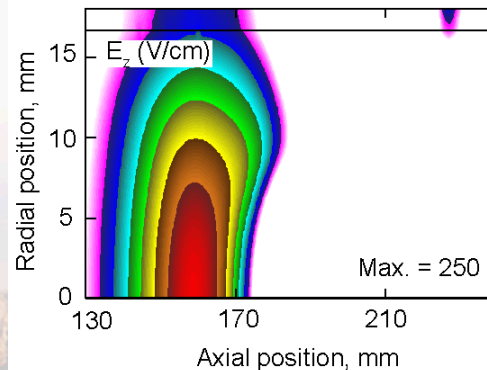
1 Torr



16 Torr



Axial field

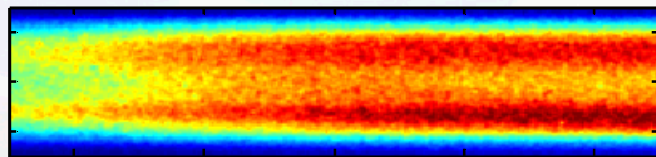
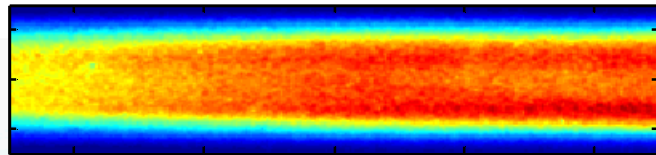
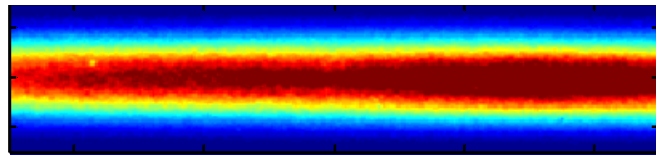


# “Unexpected” structure observed during calibration of the LCIF diagnostic

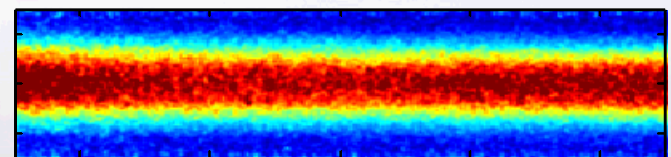
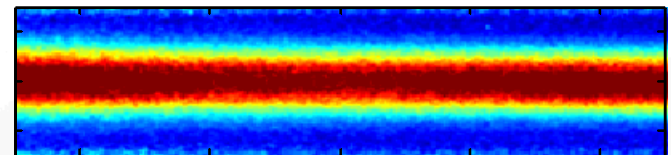
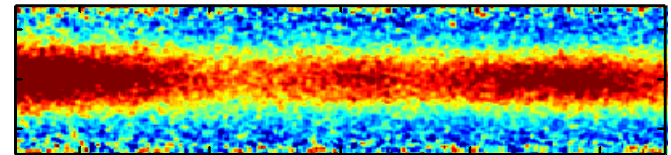
- Off-axis peak excitation is observed in  $2^3\text{P}$  species
  - Electron densities remain peaked on-axis

## Observed Behavior

$2^3\text{P}$  Distribution



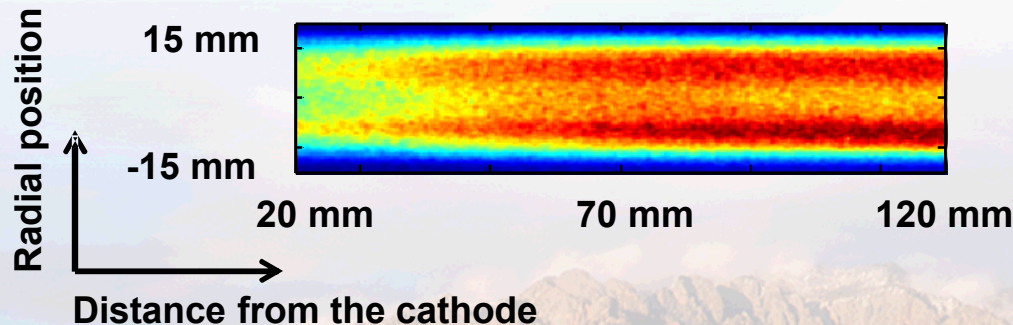
Electron Density



+5  $\mu\text{s}$

+15  $\mu\text{s}$

+25  $\mu\text{s}$



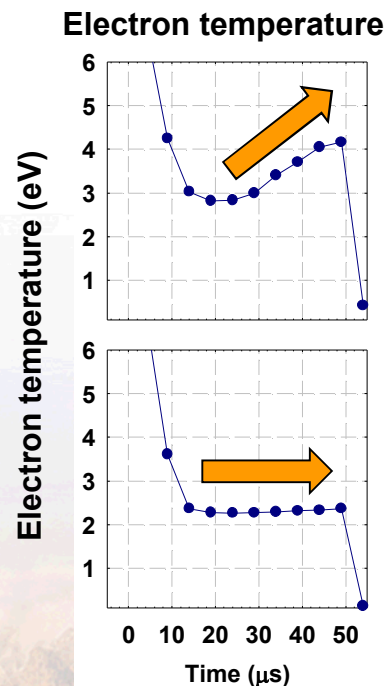
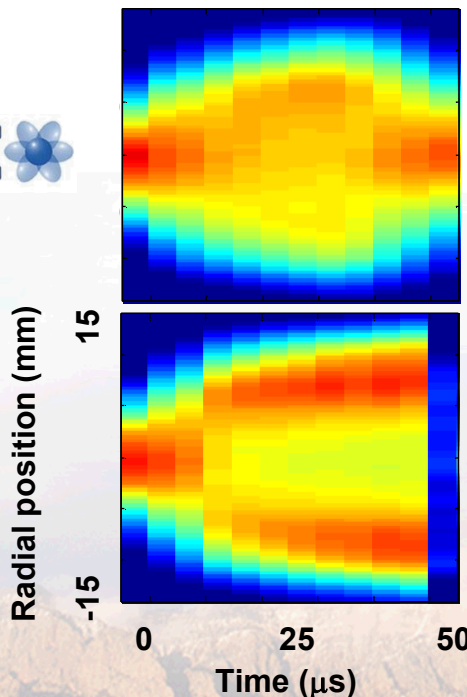
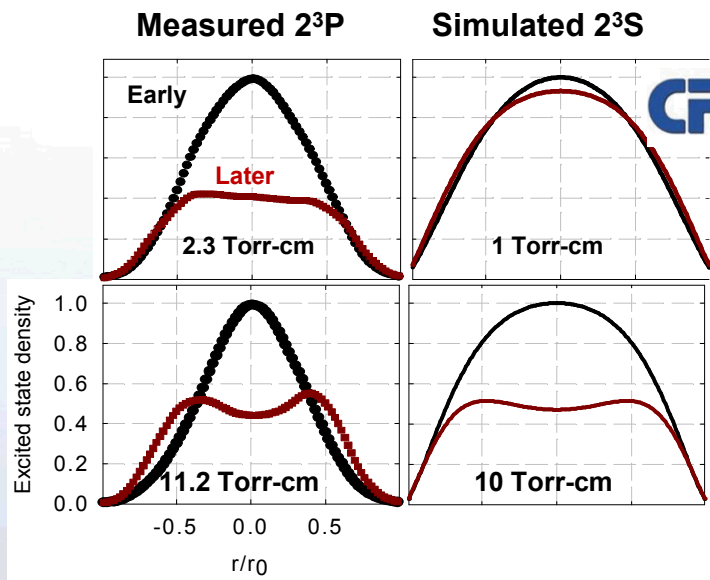
3.5 Torr Helium, 1.2 Amps



# Electron energies drive plasma structure

- Various processes were considered
  - Heating, constriction, non-linear or non-local kinetic processes
- Measurements and calculations were made to assess possibilities
  - Laser absorption to measure temperatures
  - 1D-Fluid based simulations with various “chemistries” (V. Kolobov)

## Spatial profiles

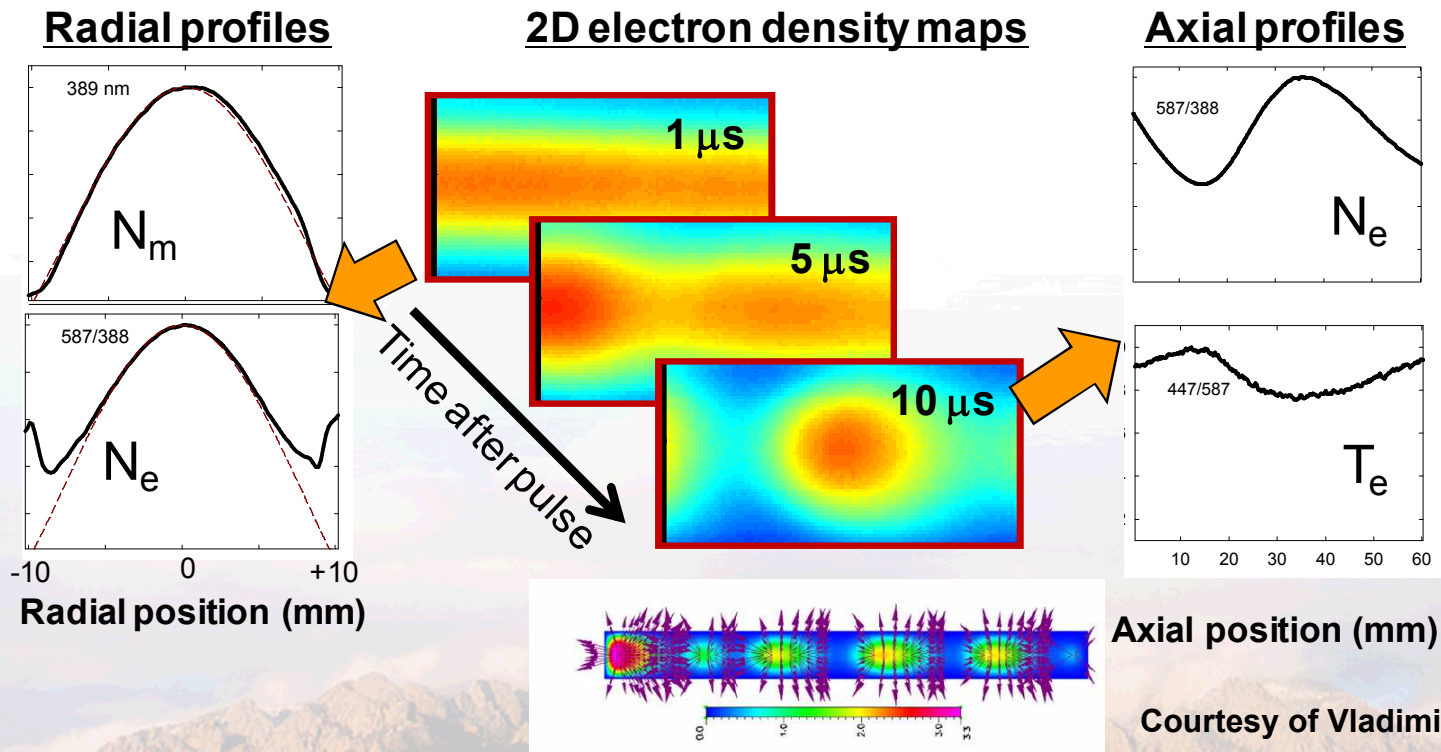
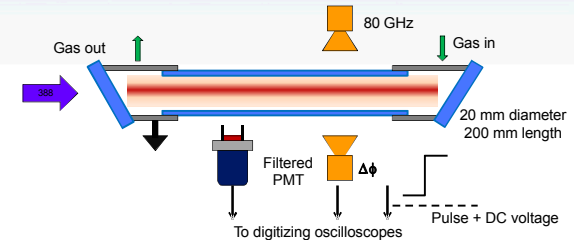


At lower pressures the both temperature and center-peaked structure are recovered; at higher pressures they are not



# LCIF is being used to study structure in a positive column

- Positive column is "well understood" system
  - Studied extensively, use it for calibration
- Platform for fast ionization wave (FIW) studies
  - Observations may warrant their own study



Courtesy of Vladimir Kolobov

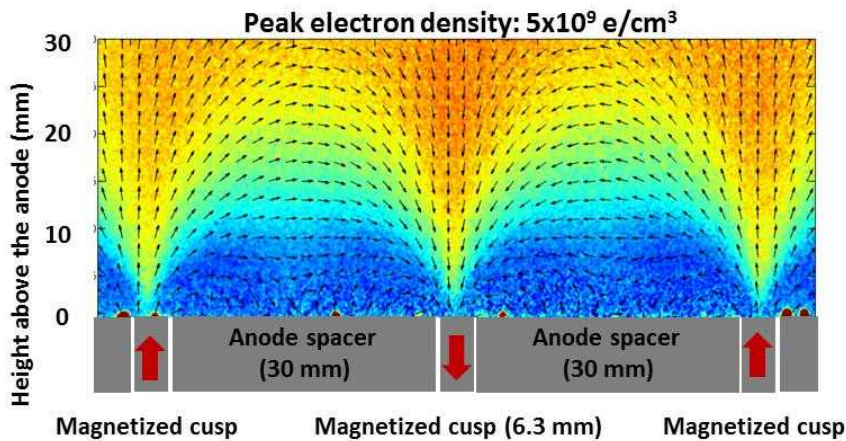
**Benchmark 2D simulations with measurements  
made by LCIF**



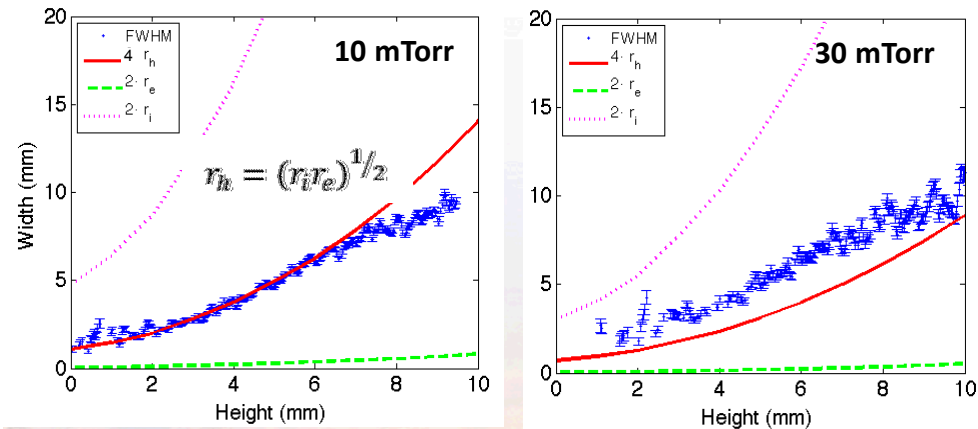
# LCIF method is utilized to look at transport in magnetized plasma

- Plasma transport in magnetized plasma is important to understand but challenging to assess
  - Magnetic configuration dictates particle balance in the plasma
- Hosted Aimee Hubble (Ph.D. candidate w/ John Foster, U. Michigan) to address fundamental questions about electron loss
  - Segmented, magnetized anode to quantify plasma confinement
  - LCIF to interrogate electron densities and measure leakage widths

## Measured electron densities



## Electron leakage widths



- Measured electron densities, temperatures and magnetic fields are used to compute leak widths

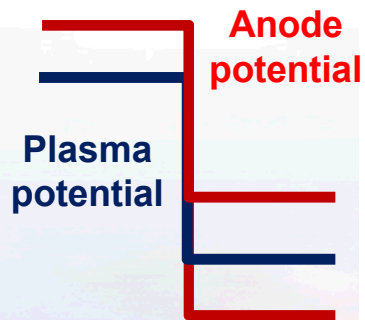
**LCIF provides non-invasive means of interrogating challenging plasma environments**



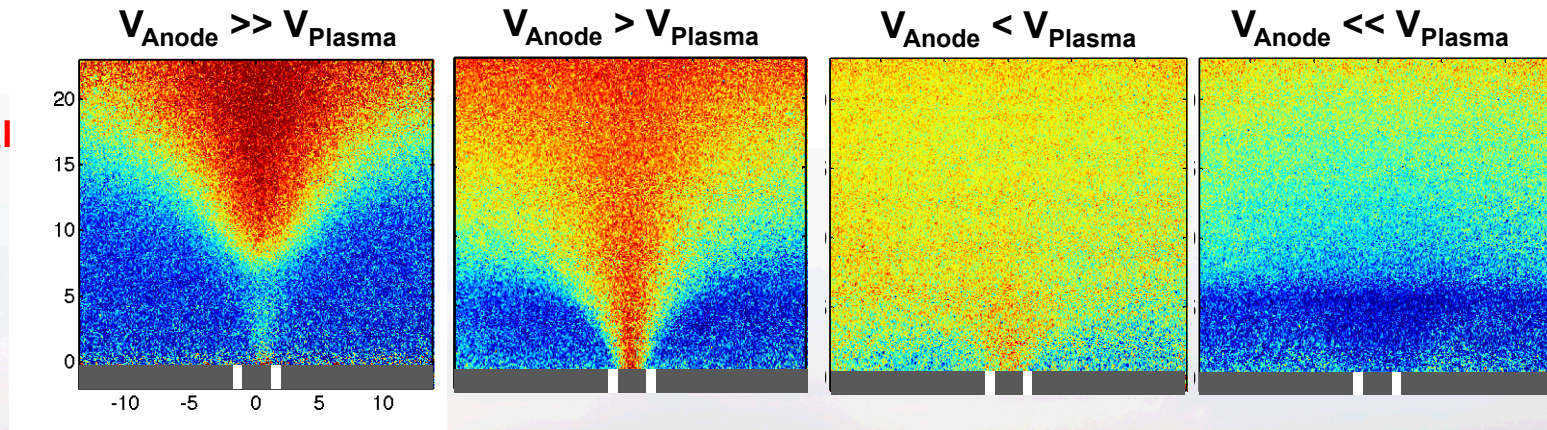
# Plasma transport is regulated by anode potential

- Transient plasma enables access to different current collecting conditions
  - Dial in potential drop between the anode and plasma
- Confinement degrades as electrode potential approaches plasma potential
  - Ion flux carries electrons across the magnetic fields

## Anode drive



## Measured electron densities

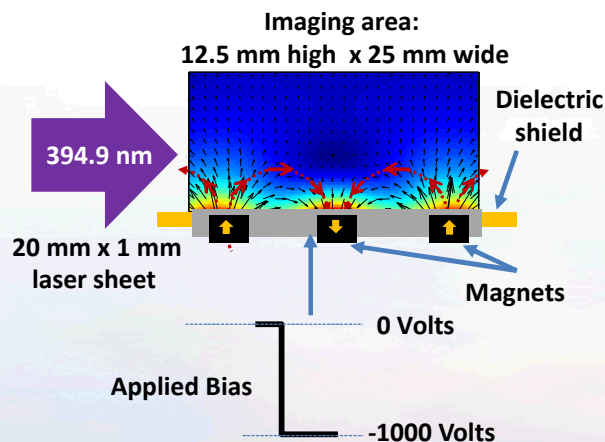


*LCIF captures plasma flow to the electrode after polarity of the bias is reversed*

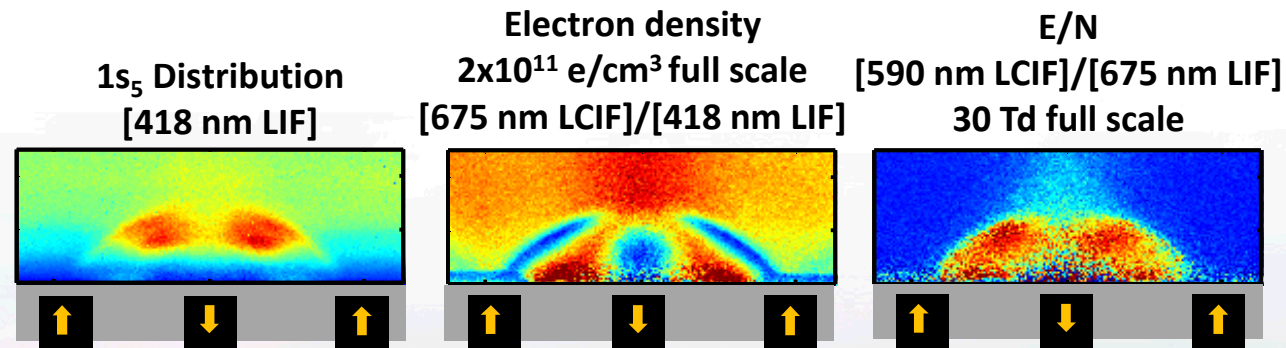
# Example of LCIF in argon environments

- Calibrated LCIF technique is applied to a transient magnetized discharge to demonstrate diagnostic capability.
  - 10 mTorr argon environment, - 1 kV pulse applied to 25 mm  $\phi$  electrode
  - Measurements acquired 1  $\mu$ s after pulse is applied

## Setup



## Observed plasma properties

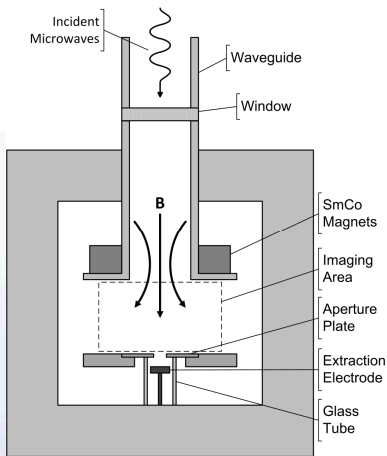


*Interesting configuration that represents challenging plasma environment that is tough to access.*

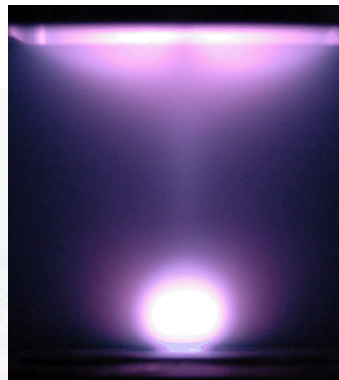
# Double layer more pronounced in ECR based plasma cathodes

- NASA driven research interested in electron sources for propulsion
  - Understand limitations on current extraction
- Host Brandon Weatherford (U. Mich.) to implement LCIF
  - Examine coupling of between plasma generation and electron extraction

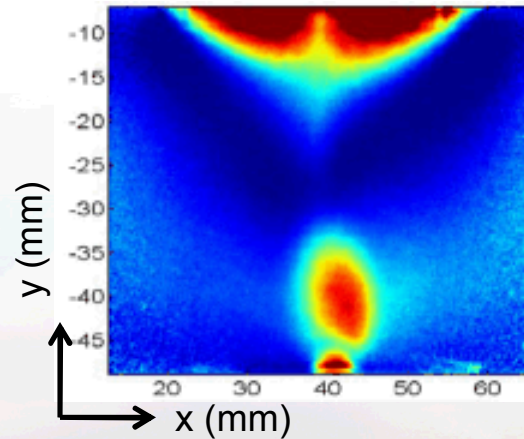
**Setup**



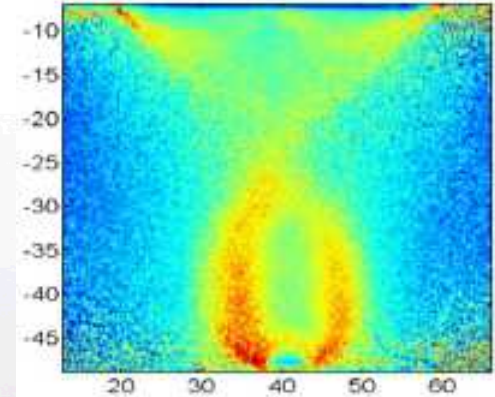
**"Full color" picture**



**Density**



**"Temperature"**



***Multi-structure plasma formed by electron-extracting electrode...  
... quite difficult to probe with more conventional means!***

# LCIF is examining anode physics and spot dynamics

- Recent studies have been focusing on anodic interfaces formed in plasma environments.
  - Rich set of physics that is uniquely different than cathodic interfaces.
  - Particularly difficult to access without perturbing the interface.
- Earlier efforts have focused on electron sheath and more recent efforts focused on spots

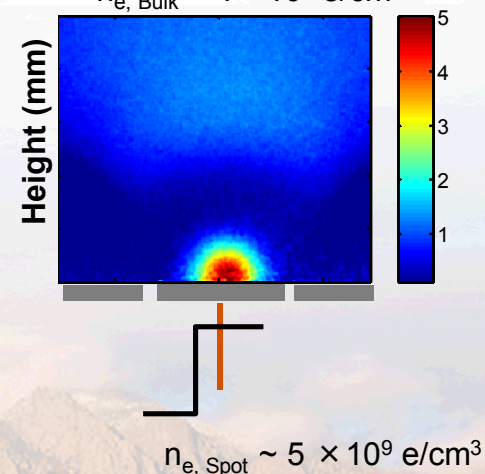
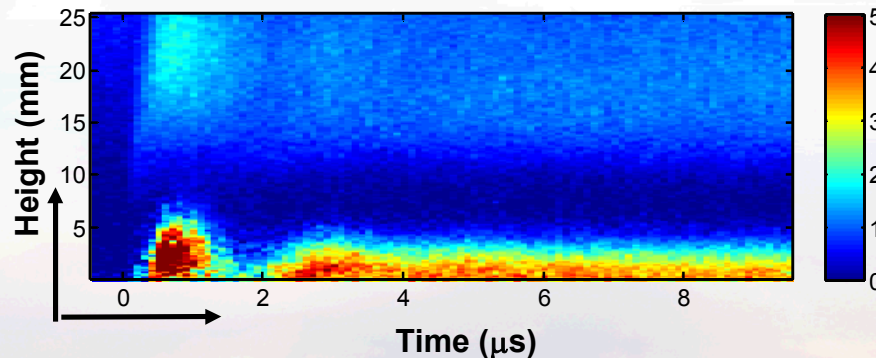
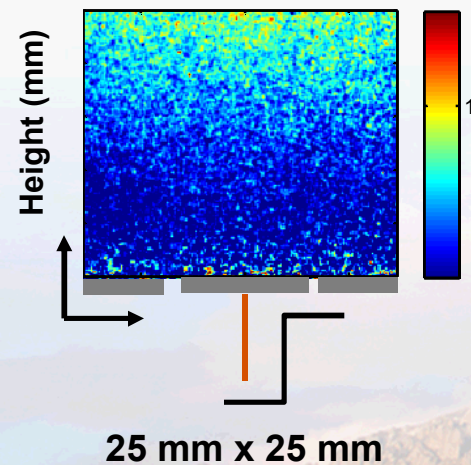
Initial plasma state:  
Electron sheath

Induced transition

Final plasma state:  
Anode spot

$n_{e, \text{Bulk}} \sim 5 \times 10^8 \text{ e/cm}^3$

$n_{e, \text{Bulk}} \sim 1 \times 10^9 \text{ e/cm}^3$



# Laser-collision induced fluorescence provides measure of electron density and "temperature"

- **Motivation: What is the density? What is the temperature? Where and When?**
  - Two-dimensional snap-shots of density provide insight into plasma physics.
- **In this presentation**
  - **Part I: Laser-collision induced fluorescence (LCIF) primer**
    - Collisional-radiative model used to predict LCIF
    - Physics that governs LCIF
  - **Part II: Implement and benchmark technique**
    - Experimental setup
    - Time evolution of LCIF and time integrated LCIF
  - **Part III: Applications of LCIF:**
    - Dynamic and structured plasmas
  - **Part IV: Future directions and concluding comments**
    - **Atmospheric pressure LCIF**





# Concluding remarks and future directions

- **LCIF technique demonstrated in 2D**
  - Free of “line of sight” constraints
  - Good spatial resolution – limited by optical collection
  - Decent temporal resolution – limited by ICCD gate times & tolerable signals
- **Caution required for proper implementation of the technique**
  - Uncertainties about rates – Absolute bounds on measurements
  - Proper choice of model – Capture the required physics
- **Technique should be extendable over broad parameter space**
  - Higher pressures – neutral collisions
  - Smaller dimensions – scattering and access
  - Other atomic systems

*This work was supported by the Department of Energy Office of Fusion Energy Science  
Contract DE-SC0001939*





# Thank you

---



# References for rates and cross-sections

## ■ Superelastic

- Klein Rosseland
- Sobelman

$$K_{ij}^e = \langle \sigma_{ij} v_e \rangle = \left( \frac{m_e}{2\pi k T_e} \right)^{3/2} \int_0^\infty \sigma_{ij}(v) \exp\left( \frac{-m_e v^2}{2k_B T_e} \right) 4\pi v^2 dv \left[ \frac{g_j}{g_i} \exp\left( \frac{(E_j - E_i)}{k_B T_e} \right) \right]$$

- [1] C. F. Burrell and H.-J. Kunze, Phys. Rev. A **18**, 2081 (1978).  
 [1] P. Chall, E. K. Souw and J. Uhlenbusch. J. Quant. Spectrosc. Radiant. Transfer **34**, 309 (1985).  
 [1] G. Dilecce, P. F. Ambrico and S. De Benedictis, J. Phys. B: At. Mol. Opt. Phys. **28**, 209 (1994).  
 [1] R. Denkelmann, S. Maurmann, T. Lokajczyk, P. Drepper, and H. -J. Kunze, J. Phys. B: At. Mol. Opt. Phys. **32**, 4635 (1999).  
 [1] R. Denkelmann, S. Freund and S. Maurmann, Contrib. Plasma Phys. **40**, 91 (2000).  
 [1] K. Tsuchida, S. Miyake, K. Kadota and J. Fujita, Plasma Physics **25**, 991 (1983).  
 [1] B. Dubreuil and P. Prigent, J. Phys. B: At. Mol. Opt. Phys. **18**, 4597 (1985).  
 [1] E. A. Den Hartog, T. R. O'Brian and J. E. Lawler, Phys. Rev. Lett. **62**, 1500 (1989).  
 [1] K. Dzierzega, K. Musiol, E. C. Benck and J. R. Roberts, J. Appl. Phys. **80**, 3196 (1996).  
 [1] L. Maleki, B. J. Blasenheim, and G. R. Janik, J. Appl. Phys. **68**, 2661 (1990).  
 [1] R. S. Stewart, D. J. Smith, I. S. Borthwick and A. M. Paterson, Phys. Rev. E **62**, 2678 (2000).  
 [1] R. S. Stewart, D. J. Smith, J. Phys. D: Appl. Phys. **35**, 1777 (2002).  
 [1] A. Hidalgo, F. L. Tabares and D. Tafalla, Plasma Phys. Control. Fusion **48**, 527 (2006).  
 [1] D. A. Shcheglov, S. I. Vetrov, I. V. Moskalenko, A. A. Skovoroda and D. A. Shuvaev, Plasma Phys. Rep. **32**, 119 (2006).  
 [1] M. Krychowiak, Ph Mertens, R. Konig, B. Schweer, S. Brezinsek, O. Schmitz, M. Brix, U. Samm and T. Klinger, Plasma Phys. Control. Fusion **50**, 65015 (2008).  
 [1] K. Takiyama, H. Sakai, M. Yamasaki, and T. Oda, Jpn. J. Appl. Phys. **33**, 5038 (1994).  
 [1] M. Watanabe, K. Takiyama, H. Toyota Jpn. J. Appl. Phys. **38**, 4380 (1999).  
 [1] G. Nersisyan, T. Morrow, and W. G. Graham, Appl. Phys. Lett. **85**, 1487 (2004).  
 [1] W. L. Wiese, M. W. Smith, and B. M. Glennon, *Atomic Transition Probabilities 4V1* (Nat. Stand. Ref. Data. Ser., Nat. Bur. Stand. Washington DC, 1966).  
 [1] Yu. Ralchenko, R. K. Janev, T. Kato, D. V. Fursa, I. Bray, F. J. De Heer, Atomic Data and Nuclear Data Tables **94**, 603 (2008).  
 [1] I.I. Sobelman, L. A. Vainshtein, and E. A. Yukov, *Excitation of Atoms and Broadening of Spectral Lines* (Springer, New York, 1981) p. 5.

$$K_{ij}^e = \langle \sigma_{ij} v_e \rangle = \left( \frac{m_e}{2\pi k T_e} \right)^{3/2} \int_0^\infty \sigma_{ij}(v) \exp\left( \frac{-m_e v^2}{2k_B T_e} \right) 4\pi v^3 dv$$

